Supporting information: Plasma-based CO$_2$ conversion: How to correctly analyze the performance?

Bart Wanten*,[1] Rani Vertongen*,[1] Robin De Meyer[1,2] and Annemie Bogaerts[1]

[1] Research group PLASMANT, Department of Chemistry, University of Antwerp, Universiteitsplein 1, 2610 Antwerp, Belgium.

[2] Research group EMAT, Department of Physics, University of Antwerp, Groenenborgerlaan 171, 2020 Antwerp, Belgium

Corresponding authors:

M. Sc Bart Wanten, email: bart.wanten@uantwerpen.be

Prof. Dr. Annemie Bogaerts, email: annemie.bogaerts@uantwerpen.be

* shared first author

S1. Formulas for pure CO$_2$ conversion: Relationships between conversion, CO$_2$/CO/O$_2$ fractions and flux ratio

The equations in Sections 2.1 and 2.2 in the main paper give the basic outline of the conversion calculation based on the fractions of CO$_2$, CO and O$_2$ (Section 2.1) as well as the relationship with the flux ratio (Section 2.2). Depending on which information is available in the experiment, the other values can be deduced, as summarized in Table S.1. For example, when we measure the CO$_2$ output fraction $y_{CO_2}^{out}$, we can obtain the conversion, by rearranging Eq. (1) in the main paper to Eq. (4) as follows:

$$y_{CO_2}^{out} = \frac{1-\chi}{1+\frac{\chi}{2}}$$

$$y_{CO_2}^{out} \cdot \left(1+\frac{\chi}{2}\right) = 1-\chi$$

$$y_{CO_2}^{out} + \frac{y_{CO_2}^{out} \cdot \chi}{2} = 1-\chi$$

$$\chi + \frac{y_{CO_2}^{out} \cdot \chi}{2} = 1-y_{CO_2}^{out}$$

$$\chi \cdot \left(1+\frac{y_{CO_2}^{out}}{2}\right) = 1-y_{CO_2}^{out}$$

$$\chi = \frac{1-y_{CO_2}^{out}}{1+\frac{y_{CO_2}^{out}}{2}}$$

Table S.1. Overview of formulas for pure CO_2 conversion: How to obtain the conversion, flux ratio, or output fraction of CO_2, CO or O_2, when one of the other values is known.

Known → Unknown ↓	χ	α	$y_{CO_2}^{out}$	y_{CO}^{out}	$y_{O_2}^{out}$
$\chi =$	χ	$2 \cdot \alpha - 2$	$\dfrac{1 - y_{CO_2}^{out}}{1 + \dfrac{y_{CO_2}^{out}}{2}}$	$\dfrac{y_{CO}^{out}}{1 - \dfrac{y_{CO}^{out}}{2}}$	$\dfrac{2 \cdot y_{O_2}^{out}}{1 - y_{O_2}^{out}}$
$\alpha =$	$1 + \dfrac{\chi}{2}$	α	$\dfrac{3}{2 + y_{CO_2}^{out}}$	$\dfrac{2}{2 - y_{CO}^{out}}$	$\dfrac{1}{1 - y_{O_2}^{out}}$
$y_{CO_2}^{out} =$	$\dfrac{1 - \chi}{1 + \dfrac{\chi}{2}}$	$\dfrac{3 - 2 \cdot \alpha}{\alpha}$	$y_{CO_2}^{out}$	$\dfrac{(y_{CO}^{out} - 2) \cdot (3 \cdot y_{CO}^{out} - 2)}{4 - 2 \cdot y_{CO}^{out}}$	$1 - 3 \cdot y_{O_2}^{out}$
$y_{CO}^{out} =$	$\dfrac{\chi}{1 + \dfrac{\chi}{2}}$	$\dfrac{2 \cdot \alpha - 2}{\alpha}$	$\dfrac{-(y_{CO_2}^{out} + 2) \cdot (y_{CO_2}^{out} - 1)}{3 + \dfrac{3 \cdot y_{CO_2}^{out}}{2}}$	y_{CO}^{out}	$2 \cdot y_{O_2}^{out}$
$y_{O_2}^{out} =$	$\dfrac{\dfrac{\chi}{2}}{1 + \dfrac{\chi}{2}}$	$\dfrac{\alpha - 1}{\alpha}$	$\dfrac{1 - y_{CO_2}^{out}}{3}$	$\dfrac{y_{CO}^{out}}{2}$	$y_{O_2}^{out}$

S2. Formulas for CO_2 conversion with a diluting agent

When adding a diluting agent to the feed gas, the dilution effect needs to be taken into account when calculating the performance metrics. When applying the same approach as described in Section 2.1 in the main paper, we obtain Table S.2. Note that these values are the flow rates of each species relative to the input CO_2 flow rate.

Table S.2. Reaction equation for pure CO_2 conversion, expressed in flow rates relative to the CO_2 flow rate at the reactor inlet, in the presence of a diluting agent.

Reaction	$CO_2 \rightarrow$	CO	O_2	Diluting agent
in	1	0	0	β
out	$1 - \chi$	χ	$\chi/2$	β

When expressing the fraction of CO_2 at the outlet, we obtain the following expression:

$$y_{CO_2}^{out} = \frac{\dot{n}_{CO_2}^{out}}{\dot{n}_{tot}^{out}} = \frac{\dot{n}_{CO_2}^{out}/\dot{n}_{CO_2}^{in}}{\dot{n}_{tot}^{out}/\dot{n}_{CO_2}^{in}} = \frac{1 - \chi}{(1 - \chi) + \chi + \frac{\chi}{2} + \beta} = \frac{1 - \chi}{1 + \frac{\chi}{2} + \beta} \tag{S.1}$$

Rearranging this equation to express conversion as function of the CO_2 output fraction is done as follows:

$$y_{CO_2}^{out} = \frac{1 - \chi}{1 + \frac{\chi}{2} + \beta}$$

$$y_{CO_2}^{out} \cdot \left(1 + \frac{\chi}{2} + \beta\right) = 1 - \chi$$

$$y_{CO_2}^{out} + \frac{y_{CO_2}^{out}}{2} \cdot \chi + y_{CO_2}^{out} \cdot \beta = 1 - \chi$$

$$\chi + \frac{y_{CO_2}^{out}}{2} \cdot \chi = 1 - y_{CO_2}^{out} - y_{CO_2}^{out} \cdot \beta$$

$$\left(1 + \frac{y_{CO_2}^{out}}{2}\right) \cdot \chi = 1 - (1 + \beta) \cdot y_{CO_2}^{out}$$

$$\chi = \frac{1 - (1 + \beta) \cdot y_{CO_2}^{out}}{1 + \frac{y_{CO_2}^{out}}{2}}$$

This is the same equation as presented by Eq. (11) in the main paper. The relationships between the conversion, the flux ratio and the CO_2, CO and O_2 fraction, as well as the fraction of the diluting agent, are presented in Table S.3.

Table S.3. Overview of formulas for pure CO_2 conversion in the presence of a diluting agent, and how to obtain the conversion, flux ratio, or output fraction of CO_2, CO, O_2 or the diluting agent, when one of the other values is known. Note that β is the dilution ratio, as defined by Eq. (10) in the main paper.

Known → Unknown ↓	χ	α	$y_{CO_2}^{out}$	y_{CO}^{out}	$y_{O_2}^{out}$	y_s^{out}
$\boldsymbol{\chi =}$	χ	$(2 \cdot \alpha - 2) \cdot (1 + \beta)$	$\dfrac{1 - (1+\beta) \cdot y_{CO_2}^{out}}{1 + \dfrac{y_{CO_2}^{out}}{2}}$	$\dfrac{(1+\beta) \cdot y_{CO}^{out}}{1 - \dfrac{y_{CO}^{out}}{2}}$	$\dfrac{2 \cdot (1+\beta) \cdot y_{O_2}^{out}}{1 - y_{O_2}^{out}}$	$\dfrac{2 \cdot \beta - 2 \cdot (1+\beta) \cdot y_s^{out}}{y_s^{out}}$
$\boldsymbol{\alpha =}$	$\dfrac{1 + \frac{\chi}{2} + \beta}{1 + \beta}$	α	$1 + \dfrac{1 - (1+\beta) \cdot y_{CO_2}^{out}}{2 \cdot (1+\beta) \cdot \left(1 + \dfrac{y_{CO_2}^{out}}{2}\right)}$	$\dfrac{2}{2 - y_{CO}^{out}}$	$\dfrac{1}{1 - y_{O_2}^{out}}$	$\dfrac{\beta}{(1+\beta) \cdot y_s^{out}}$
$\boldsymbol{y_{CO_2}^{out} =}$	$\dfrac{1 - \chi}{1 + \frac{\chi}{2} + \beta}$	$\dfrac{1 - (1+\beta) \cdot (2 \cdot \alpha - 2)}{\alpha \cdot (1+\beta)}$	$y_{CO_2}^{out}$	$\dfrac{2 - (3 + 2 \cdot \beta) \cdot y_{CO}^{out}}{2 \cdot (1+\beta)}$	$\dfrac{1 - (3 + 2 \cdot \beta) \cdot y_{O_2}^{out}}{1 + \beta}$	$\dfrac{\left(1 + 2 \cdot (1+\beta)\right) \cdot y_s^{out} - 2 \cdot \beta}{\beta}$
$\boldsymbol{y_{CO}^{out} =}$	$\dfrac{\chi}{1 + \frac{\chi}{2} + \beta}$	$\dfrac{2 \cdot \alpha - 2}{\alpha}$	$\dfrac{-(y_{CO_2}^{out} + 2) \cdot (\beta \cdot y_{CO_2}^{out} + y_{CO_2}^{out} - 1)}{\left(\frac{3}{2} + \beta\right) \cdot y_{CO_2}^{out} + 3 + 2 \cdot \beta}$	y_{CO}^{out}	$2 \cdot y_{O_2}^{out}$	$\dfrac{2 \cdot \beta - 2 \cdot (1+\beta) \cdot y_s^{out}}{\beta}$
$\boldsymbol{y_{O_2}^{out} =}$	$\dfrac{\frac{\chi}{2}}{1 + \frac{\chi}{2} + \beta}$	$\dfrac{\alpha - 1}{\alpha}$	$\dfrac{-(y_{CO_2}^{out} + 2) \cdot (\beta \cdot y_{CO_2}^{out} + y_{CO_2}^{out} - 1)}{(3 + 2 \cdot \beta) \cdot y_{CO_2}^{out} + 6 + 4 \cdot \beta}$	$\dfrac{y_{CO}^{out}}{2}$	$y_{O_2}^{out}$	$\dfrac{\beta - (1+\beta) \cdot y_s^{out}}{\beta}$
$\boldsymbol{y_s^{out} =}$	$\dfrac{\beta}{1 + \frac{\chi}{2} + \beta}$	$\dfrac{\beta}{(1 + \beta) \cdot \alpha}$	$\dfrac{\beta \cdot (2 + y_{CO_2}^{out})}{1 + 2 \cdot (1+\beta)}$	$\dfrac{\beta \cdot (2 - y_{CO}^{out})}{2 \cdot (1+\beta)}$	$\dfrac{\beta \cdot (1 - y_{O_2}^{out})}{1 + \beta}$	y_s^{out}

S3. Formulas for the reverse Boudouard reaction

The reverse Boudouard reaction (RBR) is defined as follows:

$$CO_{2\,(g)} + C_{(s)} \rightleftharpoons 2\,CO_{(g)} \tag{R.S1}$$
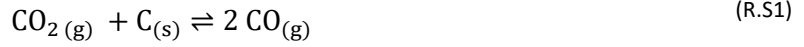
For this reaction, the standard reaction enthalpy $\Delta H°$ is equal to +172 kJ mol^{-1}, which is already 111 kJ mol^{-1} lower compared to pure CO$_2$ splitting. For more general information on the plasma-based RBR, we refer to the available literature (e.g., Refs. [1-4]).

The volumetric gas flow rate again increases and needs to be taken into account. However, with respect to using the correct formulas, the main difference with CO$_2$ splitting is that the reactants are not all in gas phase. Furthermore, because the carbon material is usually in a fixed bed positioned after the plasma, there is no fraction of carbon at the inlet and $y_{C_{(s)}}^{in}$ is zero.

Another difference is that O$_2$ will still be present in low amounts as by-product, originating from pure CO$_2$ splitting. Hence, there is some deviation from the "ideal" RBR reaction (R.S1). This means that the conversion cannot be determined solely based on the output CO$_2$ fraction $y_{CO_2}^{out}$, as was the case for pure CO$_2$ splitting. In case of the RBR, the fractions of all gaseous components need to be determined. Afterwards, the flux ratio can be derived through the O-balance equation, as all species containing O-atoms are quantified:

$$\alpha = \frac{2 \cdot y_{CO_2}^{in}}{2 \cdot y_{CO_2}^{out} + y_{CO}^{out} + 2 \cdot y_{O_2}^{out}} \tag{S.2}$$

With $y_{CO_2}^{in}$ equal to 1 if no other gas is present at the inlet. Hence, the absolute CO$_2$ conversion, O-based selectivities and yields can already be determined in the same way as described in Sections 4.2 and 4.4 of the main paper.

To derive the consumption rate of solid carbon, we write down the carbon balance equation as:

$$\frac{\alpha \cdot \left(y_{CO_2}^{out} + y_{CO}^{out}\right)}{y_{CO_2}^{in} + \dfrac{\dot{n}_{C_{(s)}}}{\dot{n}_{CO_2}^{in}}} = 1 \tag{S.3}$$

With $\dot{n}_{C_{(s)}}$ equal to the consumption or loss rate of solid carbon from the fixed bed, expressed through Eq. (S.4):

$$\dot{n}_{C_{(s)}} = \dot{n}_{CO_2}^{in} \cdot \left(\alpha \cdot \left(y_{CO_2}^{out} + y_{CO}^{out}\right) - y_{CO_2}^{in}\right) \tag{S.4}$$

The advantage of this expression is that one can follow in real-time how much carbon is consumed and from which point the bed starts to get saturated. Weighing of the carbon material before and after reaction can still serve as validation.

The "fraction" of solid carbon consumed $y_{C_{(s)}}^{in}$ is then expressed as:

$$y_{C_{(s)}}^{in} = \frac{\dot{n}_{C_{(s)}}}{\dot{n}_{C_{(s)}} + \dot{n}_{CO_2}^{in}} \tag{S.5}$$

Hence, the total conversion is defined through Eq. (S.6):

$$\chi^{\text{tot}} = y_{C_{(s)}}^{\text{in}} + \frac{\dot{n}_{CO_2}^{\text{in}}}{\dot{n}_{C_{(s)}} + \dot{n}_{CO_2}^{\text{in}}} \cdot \chi_{CO_2}^{\text{abs}} \tag{S.6}$$

The definitions for energy cost and energy efficiency remain the same as described in Section 4.3 of the main paper.

S4.   Additional details for the comparison of energy efficiency with different equations, for DRM and CO_2 hydrogenation

The numerical example in Section 5.2 of the main paper describes the different energy efficiency equations applied to a dataset for DRM in a typical warm plasma, based on earlier experiments from our group [5]. An additional numerical example for a theoretical CO_2 hydrogenation dataset in a typical cold plasma (e.g., dielectric barrier discharge) is presented below.

Table S.4. Numerical example for CO_2 hydrogenation in a typical cold plasma with a SEI = 240.6 kJ mol^{-1}: flow rates of gases at the inlet, and unreacted gases and products at the outlet.

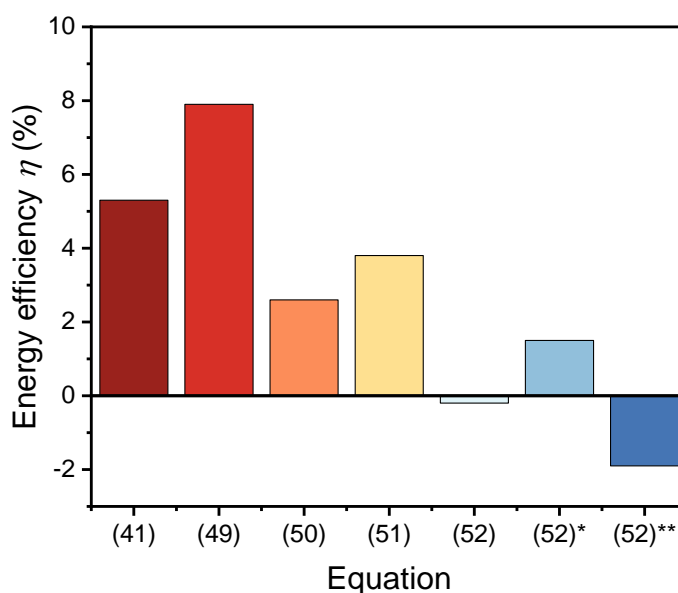| Flow rate (mL min^{-1})	CO_2	H_2	CH_4	CO	H_2O	Total
in	15	25	0	0	0	40
out	13	21.5	0.5	1.5	2.5	39

Fig. S.1. Numerical example of the energy efficiency calculated according to the various definitions for CO_2 hydrogenation. The different equation numbers refer to the equations presented in the main paper. Eq. (52)* represents the chemical energy efficiency without taking all products into account, Eq. (52)** represents the chemical energy efficiency when the reaction enthalpy corresponding to the "ideal" stoichiometry is used (described by reaction (R3) for CO_2 methanation in the main paper).

The same conclusions from the main paper remain valid for this example. In fact, due to the overall lower energy efficiency, the relative differences between the formulas are even more striking. Also note that the chemical energy efficiency (Eq. (52)) is slightly negative in this case, confirming even more that this definition is not so convenient compared to the fuel energy efficiency equations (Eqs. (41), (49), (50) and (51)).

The energy efficiency values from Fig. 2 in the main paper and Fig. S.1 are listed in Table S.5. The lower heating values, formation enthalpies and reaction enthalpies used for the calculation of the energy efficiency values are listed in Table S.6.

Table S.5. Energy efficiency values, obtained through the various equations presented in the main paper, for both the DRM (see Fig. 2 from the main paper) and CO_2 hydrogenation (Fig. S.1) numerical example.

Energy efficiency η (%)	DRM (Fig. 2 main paper)	CO_2 hydrogenation (Fig. S.1)
Eq. (41)	52.9	5.3
Eq. (49)	61.3	7.9
Eq. (50)	48.6	2.6
Eq. (51)	56.4	3.8
Eq. (52)	27.8	-0.2
Eq. (52)*	38.9	1.5
Eq. (52)**	31.3	-1.9

Table S.6. Overview of lower heating values [6], as well as the formation enthalpies & reaction enthalpies [7], used in the energy efficiency calculations.

	CO_2	0
	CH_4	802
	CO	283
	H_2	242
Lower heating values (kJ/mol)	C_2H_2	1255
	C_2H_4	1324
	C_2H_6	1428
	H_2O	0
	CO_2	-393.5
	CH_4	-74.8
	CO	-110.5
	H_2	0
Formation enthalpies (kJ/mol)	C_2H_2	226.7
	C_2H_4	52.4
	C_2H_6	-83.8
	H_2O	-241.8
Reaction enthalpy for "ideal" stoichiometry (kJ/mol)	DRM	247.3
	CO_2 methanation	-164.9

S5. Derivation of flux ratio in the presence of a standard

S5.1. CO₂ splitting

When the standard component is present as part of the feed gas, the same equations can be used as the ones presented in Table S.3 in section S2. However, when the standard is added in the exhaust stream, the flux ratio at the end, α_s, is given by:

$$\alpha_s = \frac{\dot{n}_{\text{tot}}^{\text{out}} + \dot{n}_s}{\dot{n}_{\text{tot}}^{\text{in}}} = \frac{\alpha + \beta}{1} = 1 + \frac{\chi}{2} + \beta \qquad \text{(S.7)}$$

Note that this is different from the equation in Table S.3, expressing the flux ratio as a function of conversion, due to the standard component not being present in the feed gas. As a result, all expressions for the flux ratio as a function of the conversion or one of the fractions, and vice versa, change compared to the ones presented in Table S.3. The equations to derive the flux ratio from each of the fractions are:

$$\alpha_s = 1 + \beta + \frac{1 - (1 + \beta) * y_{\text{CO}_2}^{\text{out}}}{2 + y_{\text{CO}_2}^{\text{out}}} \qquad \text{(S.8)}$$

$$\alpha_s = (1 + \beta) * \left(1 + \frac{y_{\text{CO}}^{\text{out}}}{2 - y_{\text{CO}}^{\text{out}}}\right) \qquad \text{(S.9)}$$

$$\alpha_s = (1 + \beta) * \left(1 + \frac{y_{\text{O}_2}^{\text{out}}}{1 - y_{\text{O}_2}^{\text{out}}}\right) \qquad \text{(S.10)}$$

$$\alpha_s = \frac{\beta}{y_s^{\text{out}}} \qquad \text{(S.11)}$$

Note that the equations in Table S.3 to derive the conversion from one of the measured fractions and vice versa do not change, as they are independent from the position where the standard is added. Also, it should be kept in mind that the flux ratio before the standard component is added is still defined as $1 + \frac{\chi}{2}$. The relationship between the flux ratio before (α) and after (α_s) addition of the standard can be derived from Eq. (S.7):

$$\alpha_s - \beta = 1 + \frac{\chi}{2} = \alpha \qquad \text{(S.12)}$$

Fig. S.2 shows the different stages in the gas pathway for DRM or CO_2 hydrogenation with a cold trap and GC (or any other device for gas analysis):
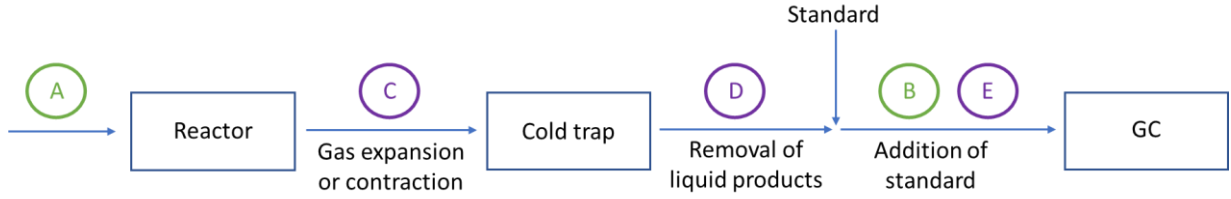

Fig. S.2. Gas pathway for a DRM/CO_2 hydrogenation experiment with cold trap and GC. The green A and B represent the initial stages (i.e. during a blank measurement, when the plasma is off) of the gas mixture, before and after dilution of the feed gas by the standard, respectively. The purple C, D and E represent the stages of the gas mixture when the plasma is on: gas expansion or contraction due to the reaction stoichiometry (C), gas contraction through removal of liquid products (D) and again dilution of the gas stream by adding the standard (E).

During the different stages of the gas pathway, the total molar and volumetric flow rate changes several times, and along with the total flow rate also the fractions of the gaseous components. When expressing a flux ratio and a fraction of a certain component, it is important to use the corresponding values, that refer to the same situations. For example, when expressing the flux ratio between situation B (flow in) and E (flow out), both the measured input and output fractions can be used directly, and the flux ratio is equal to the ratio of the obtained fractions of the standard, during the blank and plasma measurement:

$$\alpha_s^{\text{meas}} = \frac{y_s^{\text{in}}}{y_s^{\text{out}}} \tag{S.13}$$

When expressing the flux ratio between situation A (flow in) and E (flow out), the measured output fractions can still be used directly, but the measured input factors not, since they do not represent the situation at the reactor inlet where no standard is present. To account for this, the factor $(1 + \beta)$ is multiplied with the measured input fractions, as well as the flux ratio:

$$y_i^{\text{in}} = y_i^{\text{in,meas}} \cdot (1 + \beta) \tag{S.14}$$

$$\alpha_s^{\text{fin}} = \alpha_s^{\text{meas}} \cdot (1 + \beta) \tag{S.15}$$

With β still representing the dilution ratio, generally defined as:

$$\beta = \frac{\dot{n}_s}{\dot{n}_{\text{tot}}^{\text{in}}} \tag{S.16}$$

With $\dot{n}_s$ the molar flow rate of the standard s and $\dot{n}_{\text{tot}}^{\text{in}}$ the total molar flow rate at the reactor inlet. Indeed, expressing Eq. (S.15) in terms of molar flow rates becomes:

$$\alpha_s^{\text{fin}} = \frac{\dot{n}_{\text{tot}}^{\text{out}} + \dot{n}_s}{\dot{n}_{\text{tot}}^{\text{in}} + \dot{n}_s} \cdot \left(1 + \frac{\dot{n}_s}{\dot{n}_{\text{tot}}^{\text{in}}}\right) \tag{S.17}$$

With $\dot{n}_{\text{tot}}^{\text{out}}$ the total molar flow rate before addition of the standard, but after removal of liquid components (stage D in Fig. S.2). After rearrangement this results in:

$$\alpha_s^{\text{fin}} = \frac{\dot{n}_{\text{tot}}^{\text{out}} + \dot{n}_s}{\dot{n}_{\text{tot}}^{\text{in}}} \tag{S.18}$$

This proves that Eq. (S.15) represents the ratio of the flow rate in stage E relative to the flow rate in stage A. A similar derivation can be performed for Eq. (S.14) expressing the input fractions.

Note that in the main paper, we defined an "initial" flux ratio (after reaction, but before condensation/deposition of certain products) and a "final" flux ratio (after condensation/deposition of certain products) in the main paper. In this context, this corresponds with the flux ratio between stage A and C, and between A and D, respectively. The relationship between the two was given by Eq. (43) in the main paper:

$$\alpha^{\text{init}} = \frac{\alpha^{\text{fin}}}{(1 - \sum_k y_k^{\text{out}})} \tag{S.19}$$

In order to determine the initial flux ratio, the relationship between the flux ratio after condensation, but before the standard is added (α^{fin}) and the flux ratio after the standard is added (α_s^{fin}) has to be derived.

Consider again Eq. (S.17). When we divide every value by the total molar flow rate at the reactor inlet, we obtain:

$$\alpha_s^{\text{fin}} = \frac{\dfrac{\dot{n}_{\text{tot}}^{\text{out}}}{\dot{n}_{\text{tot}}^{\text{in}}} + \dfrac{\dot{n}_s}{\dot{n}_{\text{tot}}^{\text{in}}} + \dfrac{\dot{n}_s}{\dot{n}_{\text{tot}}^{\text{in}}} \cdot \left(\dfrac{\dot{n}_{\text{tot}}^{\text{out}}}{\dot{n}_{\text{tot}}^{\text{in}}} + \dfrac{\dot{n}_s}{\dot{n}_{\text{tot}}^{\text{in}}} \right)}{\dfrac{\dot{n}_{\text{tot}}^{\text{in}}}{\dot{n}_{\text{tot}}^{\text{in}}} + \dfrac{\dot{n}_s}{\dot{n}_{\text{tot}}^{\text{in}}}} \tag{S.20}$$

We can rewrite this as:

$$\alpha_s^{\text{fin}} = \frac{\alpha^{\text{fin}} + \beta + \beta \cdot \left(\alpha^{\text{fin}} + \beta \right)}{1 + \beta} \tag{S.21}$$

Note that the ratio of the total outflow over the total inflow is indeed equal to α^{fin}. This results in:

$$\alpha_s^{\text{fin}} = \alpha^{\text{fin}} + \beta \tag{S.22}$$

All expressions for the flux ratios and fractions are summarized in Table S.7. Note that a single row gives a flux ratio and an in- and output fraction that needs to be used together, when calculating each performance metric. In other words, when one uses for example the measured in- and output fractions to calculate the absolute conversion, the corresponding flux ratio (Eq. (S.13)) should be used. The only exception is the calculation of the effective conversion, where always the fraction at the reactor inlet (Eq. (S.14), corresponding to stage A in Fig. S.2) has to be used, even when the measured fractions and flux ratio are used to calculate the absolute conversion:

$$\chi_i^{\text{eff}} = y_i^{\text{in,meas}} \cdot (1 + \beta) \cdot \chi_i^{\text{abs}} = y_i^{\text{in,meas}} \cdot (1 + \beta) \cdot \frac{y_i^{\text{in,meas}} - \alpha_s^{\text{meas}} \cdot y_i^{\text{out,meas}}}{y_i^{\text{in,meas}}} \tag{S.23}$$

Using only the diluted fraction of the reactants $y_i^{\text{in,meas}}$ without the factor $(1 + \beta)$ will lead to an underestimation of the effective conversion, and hence also an underestimation of the total conversion, an overestimated energy cost, etc.

Table S.7. Expressions for flux ratio, input fraction and output fraction at each stage of the gas pathway for DRM/CO$_2$ hydrogenation. The parameters on the same row should be used together to calculate the performance metrics.

Stages	Flux ratio	Input fraction $y_i^{in} =$	Output fraction $y_{i/j}^{out} =$
In: B Out: E	$\alpha_s^{meas} = \dfrac{y_s^{in}}{y_s^{out}}$	$y_i^{in,meas}$	$y_{i/j}^{out,meas}$
In: A Out: E	$\alpha_s^{fin} = \alpha_s^{meas} \cdot (1+\beta)$	$y_i^{in,meas} \cdot (1+\beta)$	$y_{i/j}^{out,meas}$
In: A Out: D	$\alpha^{fin} = \alpha_s^{fin} - \beta$	$y_i^{in,meas} \cdot (1+\beta)$	$y_{i/j}^{out,meas} \cdot \left(1 + \dfrac{\beta}{\alpha^{fin}}\right)$
In: A Out: C	$\alpha^{init} = \dfrac{\alpha^{fin}}{1 - \sum_k y_k^{out}}$	$y_i^{in,meas} \cdot (1+\beta)$	$y_{i/j}^{out,meas} \cdot \left(1 + \dfrac{\beta}{\alpha^{fin}}\right) \cdot \left(1 - \sum_k y_k^{out}\right)$

S6. Experimental details for pure CO_2 splitting in DBD plasma

Two separate series of experiments were performed (one with a standard component, one with a flow meter) with CO_2 (Air Liquide, purity 99.999 %) flowing in a DBD plasma reactor with an input flow rate of 100 mL$_s$ min^{-1}. When using a standard, an input flow rate of 20 mL$_s$ min^{-1} N_2 was used. An Agilent 990 Micro GC was calibrated for CO_2, CO, O_2 and N_2 to analyze the fractions in the output gas mixture. The flow rate was regulated by Bronkhorst mass flow controllers, which were calibrated manually with a Sensidyne Gilibrator-3 calibrator, before the GC calibration and experiments.

For each experimental run, three samples of the input gas mixture were injected on the GC, with 5 minutes between each sample. At least eleven samples were taken of the output gas mixture, of which at least seven after reaching a steady-state. From the latter, the average of the obtained peak areas was used for further calculations. When the bubble flow meter was used, two flow rate measurements were performed for each GC sample taken. After performing these experimental runs in triplicate, the weighted averages of the performance metrics were taken. For the errors on each individual measurement, we consider both the errors on the GC calibration factors, and the standard deviation on the obtained peak areas. The plasma power was monitored and confirmed to remain constant (approximately 60 W) during the different experiments.

The output fractions of CO_2, CO, O_2 and the standard (if present), as well as the dilution factor β (obtained through the MFC calibration), the measured plasma power and specific energy input (SEI) are presented in Table S.8. Each value is a weighted average of three separate experiments. The weighted averages of the flux ratio('s) and performance metrics, calculated through the different methods, are presented in Table S.9 for the experiments with the standard, and in Table S.10 for the experiments with the flow meter.

Table S.8. Weighted averages of all measured values and the SEI (kJ/mol), for both the experiments with the standard and the flow meter.

	Standard	Flow meter
$y_{CO_2}^{out}(\%)$	73.8 ± 0.3	88.9 ± 0.4
$y_{CO}^{out}(\%)$	6.25 ± 0.02	7.34 ± 0.02
$y_{O_2}^{out}(\%)$	3.17 ± 0.02	3.58 ± 0.02
$y_s^{out}(\%)$	16.8 ± 0.2	/
β	0.211 ± 0.001	/
P (W)	59.8 ± 0.1	59.93 ± 0.06
SEI (kJ/mol)	832 ± 2	808 ± 7

Table S.9. Weighted averages of the conversion, flux ratio's, energy cost, energy yield and energy efficiency, calculated from each output fraction (incl. the standard) for the experiments performed with a standard component added.

Known → Unknown ↓	$y_{CO_2}^{out}$	y_{CO}^{out}	$y_{O_2}^{out}$	y_s^{out}
$\chi(\%) =$	7.8 ± 0.3	7.81 ± 0.02	7.93 ± 0.05	8 ± 3
$\alpha_s =$	1.250 ± 0.002	1.2496 ± 0.0006	1.2502 ± 0.0007	1.25 ± 0.02
$\alpha =$	1.039 ± 0.002	1.0391 ± 0.0009	1.0397 ± 0.0009	1.04 ± 0.02
$EC(kJ/mol) =$	$(10.6 \pm 0.4) \cdot 10^3$	$(10.65 \pm 0.04) \cdot 10^3$	$(10.49 \pm 0.07) \cdot 10^3$	$(10 \pm 4) \cdot 10^3$
$EY(mol/kJ) =$	$(9.4 \pm 0.4) \cdot 10^{-5}$	$(9.39 \pm 0.03) \cdot 10^{-5}$	$(9.53 \pm 0.07) \cdot 10^{-5}$	$(10 \pm 4) \cdot 10^{-5}$
$\eta\,(\%) =$	2.7 ± 0.1	2.66 ± 0.01	2.70 ± 0.02	3 ± 1

Table S.10. Weighted averages of the conversion, flux ratio, energy cost, energy yield and energy efficiency, calculated from each measured output fraction and the measured flux ratio for the experiments performed with a flow meter.

Known → Unknown ↓	$y_{CO_2}^{out}$	y_{CO}^{out}	$y_{O_2}^{out}$	α
$\chi(\%) =$	7.6 ± 0.3	7.61 ± 0.02	7.42 ± 0.05	7 ± 2
$\alpha =$	1.038 ± 0.001	1.0381 ± 0.0001	1.0371 ± 0.0002	1.04 ± 0.01
$EC(kJ/mol) =$	$(10.6 \pm 0.4) \cdot 10^3$	$(10.62 \pm 0.09) \cdot 10^3$	$(10.9 \pm 0.1) \cdot 10^3$	$(11 \pm 4) \cdot 10^3$
$EY(mol/kJ) =$	$(9.5 \pm 0.3) \cdot 10^{-5}$	$(9.42 \pm 0.08) \cdot 10^{-5}$	$(9.2 \pm 0.1) \cdot 10^{-5}$	$(9 \pm 3) \cdot 10^{-5}$
$\eta\,(\%) =$	2.68 ± 0.09	2.67 ± 0.02	2.60 ± 0.03	2.5 ± 0.8

S7. Experimental details for DRM in the presence of O_2, in APGD plasma

For this second example, we look at CO_2 conversion in the presence of CH_4 and O_2, specifically in a 42.5/42.5/15 CO_2/CH_4/O_2 ratio. This reaction is also called oxidative CO_2 reforming of methane (OCRM). Again, two separate series of experiments were performed (one with a standard, one with a flow meter). The gases were again provided by gas bottles from Air Liquide (purity 99.999 %), and were sent to an APGD plasma reactor through Bronkhorst MFCs, which were calibrated manually with the bubble flow meter. An Agilent 990 Micro GC was calibrated for CO_2, CH_4, CO, H_2, C_2H_2, C_2H_4, C_2H_6, O_2 and N_2 to analyze the fractions in the output gas mixture. A sample of the input gas mixture was sent three times onto the GC, with 5 minutes between each sample. The same procedure was done for the output gas mixture, after the plasma reached a steady-state. The average of the obtained peak areas was used for further calculations. Each experimental run was repeated three times, and the weighted average of the performance metrics was taken. For the errors on each individual measurement, we consider both the errors on the GC calibration factors, and the standard deviation on the obtained peak areas.

The total reactant input flow rate with the standard method was 1 $L_n min^{-1}$, and the standard was again N_2, with a flow rate of 100 $mL_n min^{-1}$ added to the effluent gas mixture between the cold trap and the GC sample point. For the experiments that were performed with the bubble flow meter, the flow rate was changed to 1 $L_s min^{-1}$. The plasma power was monitored through the readings on a DC Technix power supply, and confirmed to remain constant (91-94 W) during the different experiments.

The different fractions for each component (incl. the standard, if present), as well as the dilution ratio β (obtained through the MFC calibration), the measured plasma power and specific energy input (SEI) are presented in Table S.11 for both the experiments with the standard (left) and the flow meter (right). Each value is a weighted average of three separate experiments. The weighted averages of the flux ratios, atom balances and performance metrics, calculated through the different methods, are presented in Table S.12 for both the experiments with the standard (left) and the flow meter (right).

Table S.11. Weighted averages of all measured values and the SEI (kJ/mol), for both the experiments with the standard and the flow meter.

	Standard	Flow meter
$y_{CO_2}^{in}$ (%)	38.4 ± 0.2	43.0 ± 0.2
$y_{CH_4}^{in}$ (%)	38.3 ± 0.1	42.2 ± 0.2
$y_{O_2}^{in}$ (%)	14.41 ± 0.03	16.05 ± 0.03
y_s^{in} (%)	9.37 ± 0.02	/
$y_{CO_2}^{out}$ (%)	17.7 ± 0.2	17.5 ± 0.2

$y_{CH_4}^{out}$ (%)	8.9 ± 0.2	8.7 ± 0.3
$y_{O_2}^{out}$ (%)	1.6 ± 0.1	1.5 ± 0.1
y_{CO}^{out} (%)	34.3 ± 0.3	40.0 ± 0.3
$y_{H_2}^{out}$ (%)	28.5 ± 0.2	31.5 ± 0.3
$y_{C_2H_2}^{out}$ (%)	1.31 ± 0.02	1.41 ± 0.03
$y_{C_2H_4}^{out}$ (%)	0.376 ± 0.008	0.389 ± 0.007
$y_{C_2H_6}^{out}$ (%)	0.0929 ± 0.0006	0.0800 ± 0.0006
y_s^{out} (%)	7.57 ± 0.07	/
β	0.0977 ± 0.0004	/
P (W)	91.3 ± 0.9	94 ± 1
SEI (kJ/mol)	117 ± 1	127 ± 2

Table S.12. Weighted averages of all calculated values based on the different methods, for both the experiments with the standard and the flow meter.

	Stoichiometric	Standard	Stoichiometric	Flow meter
α_s^{meas}	1.102 ± 0.008	1.24 ± 0.01	/	/
α_s^{fin}	1.307 ± 0.009	1.36 ± 0.01	/	/
α^{fin}	1.209 ± 0.009	1.26 ± 0.01	1.23 ± 0.01	1.24 ± 0.01
α^{init}	1.42 ± 0.01	1.43 ± 0.02	1.45 ± 0.01	1.45 ± 0.02

$\chi_{CO_2}^{abs}$ (%)	45.2 ± 0.8	43.1 ± 0.8	49.9 ± 0.8	49.0 ± 0.9
$\chi_{CH_4}^{abs}$ (%)	72.3 ± 0.6	71.3 ± 0.6	74.9 ± 0.8	74.6 ± 0.9
$\chi_{O_2}^{abs}$ (%)	87 ± 1	86 ± 1	88.3 ± 0.9	88.1 ± 0.9
$\chi_{CO_2}^{eff}$ (%)	19.1 ± 0.4	18.2 ± 0.4	21.4 ± 0.4	21.1 ± 0.4
$\chi_{CH_4}^{eff}$ (%)	30.4 ± 0.3	29.9 ± 0.3	31.6 ± 0.4	31.5 ± 0.4
$\chi_{O_2}^{eff}$ (%)	13.7 ± 0.2	13.6 ± 0.2	14.2 ± 0.2	14.1 ± 0.2
χ^{tot} (%)	63.1 ± 0.5	61.7 ± 0.5	67.4 ± 0.6	66.9 ± 0.6
S_{CO}^{C} (%)	91 ± 2	97 ± 2	92 ± 2	93 ± 2
$S_{C_2H_2}^{C}$ (%)	6.9 ± 0.2	7.4 ± 0.2	6.4 ± 0.2	6.6 ± 0.2
$S_{C_2H_4}^{C}$ (%)	1.99 ± 0.05	2.12 ± 0.06	1.82 ± 0.05	1.86 ± 0.06
$S_{C_2H_6}^{C}$ (%)	0.491 ± 0.009	0.52 ± 0.01	0.365 ± 0.007	0.38 ± 0.01
$S_{H_2}^{H}$ (%)	61 ± 1	65 ± 1	61 ± 1	62 ± 1
$S_{C_2H_2}^{H}$ (%)	2.82 ± 0.06	2.97 ± 0.06	2.70 ± 0.07	2.75 ± 0.07
$S_{C_2H_4}^{H}$ (%)	1.63 ± 0.04	1.71 ± 0.04	1.51 ± 0.04	1.54 ± 0.04
$S_{C_2H_6}^{H}$ (%)	0.600 ± 0.009	0.63 ± 0.01	0.459 ± 0.009	0.47 ± 0.01
$S_{H_2O}^{H}$ (%)	34.3 ± 0.05	28.7 ± 0.5	35 ± 2	33.4 ± 0.7

$S_{CO}^{O}(\%)$	68 ± 1	73 ± 1	68 ± 1	70 ± 1
$S_{H_2O}^{O}(\%)$	31.7 ± 0.4	26.9 ± 0.4	32 ± 2	30.1 ± 0.6
$Y_{CO}^{C}(\%)$	53.1 ± 0.6	55.0 ± 0.7	57.4 ± 0.7	57.9 ± 0.9
$Y_{C_2H_2}^{C}(\%)$	4.05 ± 0.07	4.21 ± 0.07	4.03 ± 0.09	4.1 ± 0.1
$Y_{C_2H_4}^{C}(\%)$	1.17 ± 0.03	1.21 ± 0.03	1.12 ± 0.02	1.13 ± 0.03
$Y_{C_2H_6}^{C}(\%)$	0.288 ± 0.003	0.299 ± 0.004	0.231 ± 0.003	0.235 ± 0.004
$Y_{H_2}^{H}(\%)$	44.3 ± 0.5	45.9 ± 0.5	45.9 ± 0.6	46.5 ± 0.7
$Y_{C_2H_2}^{H}(\%)$	2.03 ± 0.04	2.11 ± 0.04	2.03 ± 0.05	2.06 ± 0.05
$Y_{C_2H_4}^{H}(\%)$	1.17 ± 0.03	1.21 ± 0.03	1.13 ± 0.02	1.14 ± 0.03
$Y_{C_2H_6}^{H}(\%)$	0.433 ± 0.005	0.449 ± 0.005	0.350 ± 0.005	0.356 ± 0.006
$Y_{H_2O}^{H}(\%)$	24.7 ± 0.3	20.0 ± 0.3	27 ± 2	25.1 ± 0.5
$Y_{CO}^{O}(\%)$	38.6 ± 0.5	40.0 ± 0.5	41.4 ± 0.5	41.8 ± 0.6
$Y_{H_2O}^{O}(\%)$	17.9 ± 0.2	14.5 ± 0.2	19 ± 1	17.9 ± 0.3
b_C	1.00 ± 0.01	1.04 ± 0.01	1.00 ± 0.01	1.01 ± 0.01
b_H	1.01 ± 0.01	0.99 ± 0.01	1.01 ± 0.02	1.00 ± 0.01
b_O	1.00 ± 0.01	1.00 ± 0.01	1.00 ± 0.02	1.00 ± 0.01

EC (**kJ/mol**)	179 ± 3	183 ± 3	186 ± 3	188 ± 3
EY (**mol/kJ**)	$(5.60 \pm 0.08) \cdot 10^{-3}$	$(5.47 \pm 0.08) \cdot 10^{-3}$	$(5.37 \pm 0.09) \cdot 10^{-3}$	$(5.33 \pm 0.09) \cdot 10^{-3}$
η (%) (**Eq. (41)**)	54.8 ± 0.6	56.7 ± 0.6	56.2 ± 0.6	56.9 ± 0.8
η (%) (**Eq. (49)**)	69.4 ± 0.9	73 ± 1	68 ± 1	70 ± 1
η (%) (**Eq. (50)**)	48.2 ± 0.5	49.9 ± 0.5	50.0 ± 0.6	50.6 ± 0.7
η (%) (**Eq. (51)**)	61.0 ± 0.8	63.9 ± 0.9	60.7 ± 0.9	62 ± 1
η (%) (**Eq. (52)**)	2 ± 1	5 ± 1	3 ± 3	3 ± 2

S8. References

[1] F. Girard-Sahun, O. Biondo, G. Trenchev, G.J. van Rooij, A. Bogaerts, Carbon bed post-plasma to enhance the CO2 conversion and remove O2 from the product stream, Chemical Engineering Journal 442 (2022) 136268. https://doi.org/10.1016/j.cej.2022.136268.

[2] J. Huang, H. Zhang, Q. Tan, L. Li, R. Xu, Z. Xu, X. Li, Enhanced conversion of CO2 into O2-free fuel gas via the Boudouard reaction with biochar in an atmospheric plasmatron, Journal of CO2 Utilization 45 (2021). https://doi.org/10.1016/j.jcou.2020.101429.

[3] Y. Wu, S.-Z. Li, Y.-L. Niu, H. Yan, D. Yang, J. Zhang, Experimental investigation of CO2 conversion in Boudouard reaction driven by an atmospheric-pressure microwave plasma torch, Journal of Physics D: Applied Physics (2022). https://doi.org/10.1088/1361-6463/acaeda.

[4] H. Zhang, Q. Tan, Q. Huang, K. Wang, X. Tu, X. Zhao, C. Wu, J. Yan, X. Li, Boosting the Conversion of CO2 with Biochar to Clean CO in an Atmospheric Plasmatron: A Synergy of Plasma Chemistry and Thermochemistry, ACS Sustainable Chemistry & Engineering 10(23) (2022) 7712-7725. https://doi.org/10.1021/acssuschemeng.2c01778.

[5] B. Wanten, S. Maerivoet, C. Vantomme, J. Slaets, G. Trenchev, A. Bogaerts, Dry reforming of methane in an atmospheric pressure glow discharge: Confining the plasma to expand the performance, Journal of CO2 Utilization 56 (2022) 101869. https://doi.org/10.1016/j.jcou.2021.101869.

[6] T.E. Toolbox, Gases - Gross and Net Heat Values, 2003. https://www.engineeringtoolbox.com/gross-net-heating-values-d_420.html. (Accessed 25 April 2023).

[7] B. Szyk, D. Czernia, Enthalpy Calculator. https://www.omnicalculator.com/physics/enthalpy. (Accessed 25 April 2023).